Designing Behaviors to Improve Observability for Relative Localization of AUVs

Gianluca Antonelli, Andrea Caiti, Vincenzo Calabrò, Stefano Chiaverini

Abstract— **Coordinated control of marine vehicles poses challenging problems, among them the possibility to use the vehicles, in addition to their nominal mission, also to achieve a relative localization task. To the purpose, the use of a surface, GPS-equipped, vehicle and one or several underwater vehicles may be envisaged. The latters can communicate among them by acoustic modems; those devices can also be used as ranging measurement units thus providing an additional information that, together with the common sensor equipment for marine vehicles, might be used for relative localization. This paper investigates how the vehicles' movements can be commanded in order to help the relative localization by a proper analysis of the system observability and a corresponding proper definition of the vehicles movements; critical situations for the relative observability, that corresponds to common movements, are then avoided. Numerical simulations on the mathematical model of the Fòlaga hybrid underwater vehicle confirm the effectiveness of the proposed coordinated behavioral approach.**

I. INTRODUCTION

Localization of an underwater vehicle is a demanding task. It is well known, in fact, that technologies such as GPS (Global Positioning System) can not be used. An AUV (Autonomous Underwater Vehicle) is usually equipped with several sensors but none of them may provide its position with respect to an inertial frame. Currently, the most diffused localization strategy is achieved by the use of an external array of acoustic baseline; the drawback of such an approach relies in the high cost and the bounded space covered by the array, usually confined in few kilometers. An alternative is given by IMUs (Inertial Measurement Units) that provide the position by proper integration of velocity/acceleration information; to achieve satisfactory results very expensive should be acquired.

Recently, the use of several autonomous, both surface and underwater vehicles, received attention from the research community. The vehicles might coordinate their movements, eventually communicate via acoustic modems such as the one described in [18], thus allowing to design autonomous missions that can not be afforded by one single vehicle.

The work [7] uses multiple vehicles to perform localization and found the solution by building, at each sample time, all the possible solutions to the localization problem and selecting the most appropriate via the minimization of

Authors are in alphabetical order.

Gianluca Antonelli and Stefano Chiaverini are with the Dipartimento di Automazione, Elettromagnetismo, Ingegneria dell'Informazione e Matematica Industriale, Università degli Studi di Cassino, Via G. Di Biasio 43, 03043, Cassino (FR), Italy, {antonelli,chiaverini}@unicas.it.

Andrea Caiti and Vincenzo Calabrò are with the Dipartimento di Sistemi Elettrici e Automazione, Università di Pisa, Via Diotisalvi, 2, 56126, Pisa, Italy {andrea.caiti,v.calabro}@dsea.unipi.it.
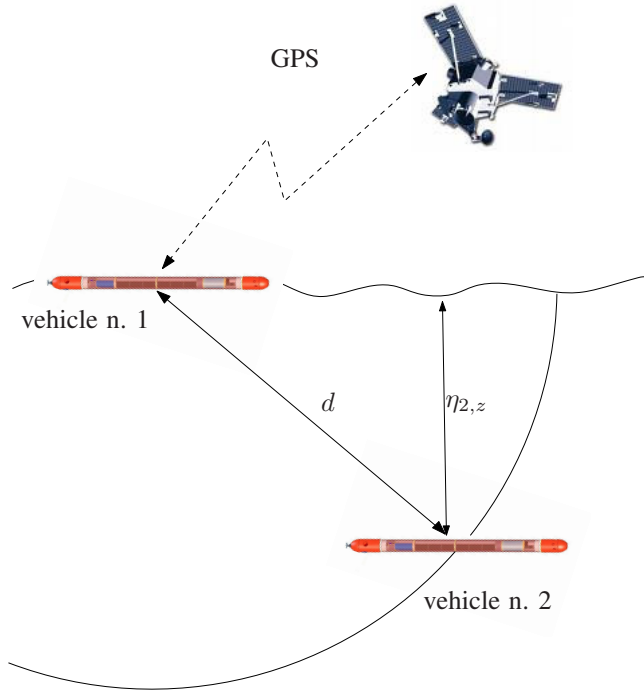
a proper cost function. Interesting experimental results are presented in different scenarios, in one of them, in addition, the use of surface test vehicles equipped with GPS gives also ground truth data; the observability, however, is not object of study. Similarly to [7], in [15], a proper filter, in this case Kalman-based, is build in order to implement cooperative localization, experimental results are provided. In [12], the bearing and the distance are used to achieve relative localization; the relative bearing, however, is not available with an off-the-shelf acoustic modem, in [12], in fact, the use of two wide-band acoustic pulses together with two hydrophones for each vehicle is required. In [14], one single vehicle, measuring its distance from a GPS-equipped transponder, is used to show the concept of *synthetic* long baseline localization.

It is thus interesting to merge the two problems above, localization and coordination by properly programming the vehicles in order to implement relative localization algorithm and avoid *singular* configurations in which those fail or, on the other hand, by adopting proper behaviors that improve relative *observability*. Figure 1 gives a sketch of the localization algorithm, one vehicle, equipped with a GPS, is traveling at the surface while one or more vehicles, coordinated with it, are traveling under the water. The vehicle can communicate via acoustic modems and thus they can measure the relative distance. The investigation presented in this paper concerns the mobility of the Fòlaga vehicle [1], a low cost marine vehicle with mixed characteristics of a glider and an AUV.

II. OBSERVABILITY ANALYSIS

A detailed observability analysis, including concepts of local weak observability for non-linear systems [19], is out of the scope of this paper, some recent results can be found in [8] or [4]. In this paper the sole observability matrices will be reported and discussed in order to focus on the behavioral control aspect of the problem.

Let $\Sigma_I : \{O - xyz\}$ be an inertial, earth-fixed, reference frame and let $\Sigma_{v,i} : \{O_{v,i} - x_{v,i}y_{v,i}z_{v,i}\}$ be the vehicle-fixed frame of the i-th vehicle. The unit vector z is parallel to gravity, $x_{v,i}$ is parallel to the vehicle fore-aft direction, and $z_{v,i}$ is aligned with z when the vehicle is neutrally leveled. The vector $\eta_i \in \mathbb{R}^3$ represents the vehicle position, i.e., the coordinate of the origin of frame $\Sigma_{v,i}$ in the inertial reference system Σ_I.

The kinematic equations representing the relative motion of one vehicle with respect to the other are given by

$$\dot{p} = -v_1 + R_2^1 v_2 - S(\omega_1)p \qquad (1)$$

Fig. 1. Sketch of the cooperative localization scenario.

where $\boldsymbol{p} \in \mathbb{R}^3$ is the position of the second vehicle with respect to the first vehicle expressed in frame 1, the vector $\boldsymbol{v}_i \in \mathbb{R}^3$ with $i = \{1, 2\}$ is the linear velocity of the frame origin expressed in its own frame, the vector $\boldsymbol{\omega}_1$ is the angular velocity of the frame origin expressed in its own frame, the matrix $\boldsymbol{S}(\boldsymbol{\zeta})$ defined as

$$\boldsymbol{S}(\boldsymbol{\zeta}) = \begin{bmatrix} 0 & -\zeta_z & \zeta_y \\ \zeta_z & 0 & -\zeta_x \\ -\zeta_y & \zeta_x & 0 \end{bmatrix} \quad (2)$$

is the skew symmetric matrix performing the cross product operation and finally the matrix $\boldsymbol{R}_2^1 \in \mathbb{R}^{3 \times 3}$ is the rotation matrix from frame 2 to frame 1. Figure 2 illustrates the relationship among the main variables above.
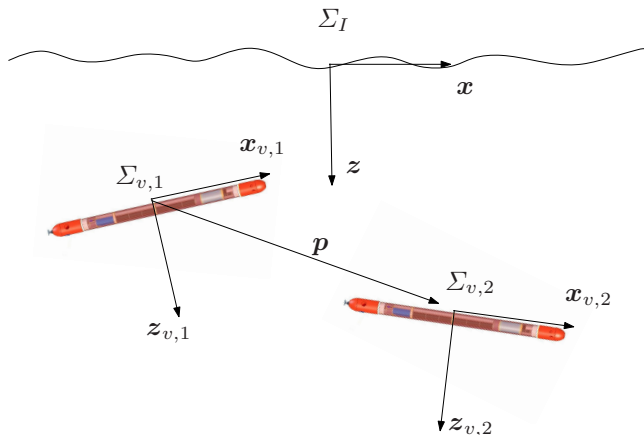

Fig. 2. Sketch of the kinematic variables.

Assuming a common sensor suite for each of the vehicles means that the linear and angular velocities, the vehicle rotations and the depth are measurable, in addition, a ranging measurement is also available. The output vector is then defined as

$$\boldsymbol{y} = \begin{bmatrix} \frac{1}{2}\boldsymbol{p}^{\mathrm{T}}\boldsymbol{p} \\ \eta_{2,z} - \eta_{1,z} \end{bmatrix} \quad (3)$$

where, as suggested in [19], for the first output the square of the distance is used instead of the distance itself to simplify the following computations. It is worth noticing, moreover, that for the second output the following holds:

$$\eta_{2,z} - \eta_{1,z} = \begin{bmatrix} 0 & 0 & 1 \end{bmatrix} \boldsymbol{R}_1^I \boldsymbol{p}. \quad (4)$$

Defining as $\boldsymbol{p}$ the system state the following nonlinear continuous-time dynamic system is obtained:

$$\begin{cases} \dot{\boldsymbol{p}} = & \boldsymbol{f}(\boldsymbol{p}, \boldsymbol{u}) \\ \boldsymbol{y} = & \boldsymbol{h}(\boldsymbol{p}) \end{cases} \quad (5)$$

for which an estimate $\hat{\boldsymbol{p}}$ needs to be designed.

The observability matrix $\boldsymbol{O} \in \mathbb{R}^{6 \times 3}$ of the linearized system is given by [4]

$$\boldsymbol{O} = \begin{bmatrix} \boldsymbol{p}^{\mathrm{T}} \\ \boldsymbol{z}_{v,1}^{I \ \mathrm{T}} \\ -\boldsymbol{p}^{\mathrm{T}}\boldsymbol{S}(\omega_1) \\ -\boldsymbol{z}_{v,1}^{I \ \mathrm{T}}\boldsymbol{S}(\omega_1) \\ \boldsymbol{p}^{\mathrm{T}}\boldsymbol{S}(\omega_1)^2 \\ \boldsymbol{z}_{v,1}^{I \ \mathrm{T}}\boldsymbol{S}(\omega_1)^2 \end{bmatrix}. \quad (6)$$

Given the non-linear system in eq. (5) more advanced mathematical tools aimed at study observability for non-linear systems may be required such as the concept of *local weak observability* introduced in [11]. The observability matrix $\mathcal{O}$ for the latter property becomes [4]

$$\mathcal{O} = \begin{bmatrix} \boldsymbol{p}^{\mathrm{T}} \\ \boldsymbol{z}_{v,1}^{I \ \mathrm{T}} \\ [-\boldsymbol{v}_1 + \boldsymbol{R}_2^1\boldsymbol{v}_2]^{\mathrm{T}} \\ -\boldsymbol{z}_{v,1}^{I \ \mathrm{T}}\boldsymbol{S}(\omega_1) \\ [-(-\boldsymbol{v}_1 + \boldsymbol{R}_2^1\boldsymbol{v}_2)\boldsymbol{S}(\omega_1)]^{\mathrm{T}} \\ \boldsymbol{z}_{v,1}^{I \ \mathrm{T}}\boldsymbol{S}(\omega_1)^2 \\ \vdots \end{bmatrix}. \quad (7)$$

Independently from the specific filter implemented, study of the rank of the matrices above is of fundamental importance since it gives the *measure* of how confident one should be on the output of the filter used to estimate $\boldsymbol{p}$. It is known, in fact, that an EKF (Extended Kalman Filter) might be used for a system whose linearized model is observable, with small noise and small initial error [13], [16]; on the other hand, the local weak observability can be made full rank in wider conditions but it does not give a systematic procedure to design a proper filter.

A. Effect of common AUVs' movements

Assuming the mission starting with both vehicles at the surface, to reach the configuration depicted in Figure 1, the Fòlaga is usually commanded to dive by deflating air maintaining null pitch and roll angles as shown in Figure 3.
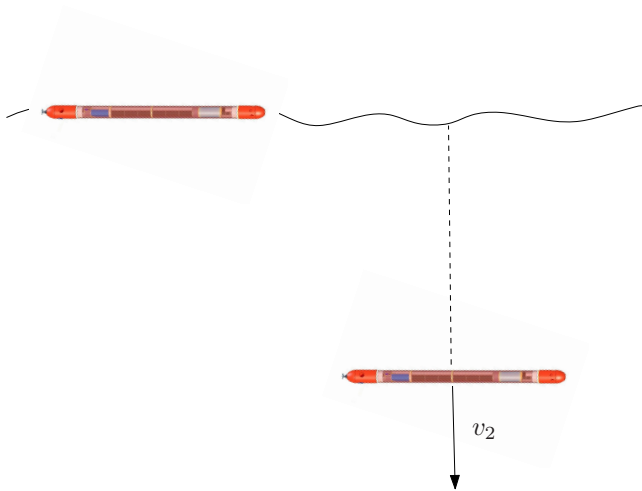

Fig. 3. Typical dive for a Fòlaga vehicle, deflating air allows the vehicle to dive with null roll and pitch angles.

By visual inspection of the observability matrix for the linearized system reported in eq. (6) it can be verified that, being $\boldsymbol{\omega}_1 = \mathbf{0}$, the rank is at maximum 2. Moreover, it can be unitary if the dive's path is aligned with $\boldsymbol{z}_{v,1}$ and it has null roll and pitch angles too. During such a dive, moreover, the term $-\boldsymbol{v}_1 + \boldsymbol{R}_2^1 \boldsymbol{v}_2$ is parallel to the vector $\begin{bmatrix} 0 & 0 & 1 \end{bmatrix}^{\mathrm{T}}$ and thus even the local weak observability is not guaranteed. Even if the initial error is small, e.g., also the second vehicle is GPS-equipped, during such a dive the designed filter might increase the estimation error without proof of boundedness.

Another common movement concerning the two vehicles is sketched in Figure 4, here the vehicles move at the same speed and direction. Again, the observability of the linearized system is not verified. For the local weak observability it is interesting to notice that the third row $-\boldsymbol{v}_1 + \boldsymbol{R}_2^1 \boldsymbol{v}_2$ represents the velocity of the second vehicle, *as seen from the first vehicle*, expressed in the frame of the first vehicle. If the two vehicles travel with the same velocity their relative velocity is null and, being $\boldsymbol{\omega}_1 = \mathbf{0}$, even the local weak observability is lost.

In general, it is clear that the observability of the linearized system requires, at least, one component of the angular velocity different from zero while the local weak observability may be achieved even for $\boldsymbol{\omega}_1 = \mathbf{0}$.

It is interesting to customize the observability considerations for a couple of AUVs travelling on a configuration such as the one shown in figure 1, i.e., with one vehicle at the surface. The only not null angular velocity component of the first vehicle is usually $\omega_{1,z}$ and thus the vector $\boldsymbol{\omega}_1$ is parallel to $\begin{bmatrix} 0 & 0 & 1 \end{bmatrix}$. A coordinated movement, i.e., a proper definition of the relative movement between the two
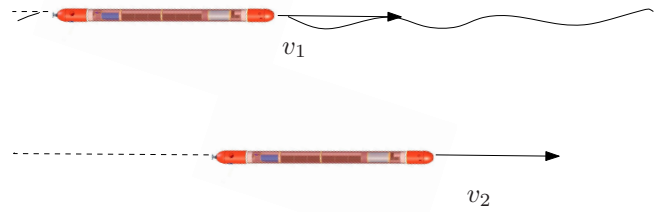

Fig. 4. The two vehicles travelling on their corresponding planes with the same velocity corresponds to a low-rank observability scenario.

vehicles, thus, including a non-null rotation, might avoid the loss of observability for the localization problem.

Observing the nonlinear system and its observability characteristics, however, one interesting difference with respect to the linearized model is given by the presence of the linear velocity in the matrix $\mathcal{O}$. This gives an additional possibility to try to achieve observable configurations by properly selecting the inputs. Moreover, by visual inspection of the first three rows it is already possible to find a sufficient condition to ensure the local weak observability property. The third line represent the velocity of the second vehicle, *as seen from the first vehicle*, expressed in the frame of the first vehicle. It is sufficient that this relative velocity is not a linear combination of z_I and $\boldsymbol{p}$ and, obviously, is not null either. Differently from the previous case, thus, a local weak observability can be achieved without inspecting the angular velocities that can be eventually null.

III. BEHAVIORAL CONTROL TO IMPROVE OBSERVABILITY

Behavioral control is a diffused approach to handle autonomous robots, see, e.g., the Arkin's textbook [6] for an interesting discussion on this topic. Among the behavioral approaches, seminal works are reported in the papers [9] and [5]; in this paper, the approach proposed in [3], defined NSB (Null-Space-base Behavioral) control will be used. The NSB approach is priority-based and it has some advantages with respect to the cooperative or competitive behavioral approaches, namely:

- Priorities are strictly guaranteed;
- Rigorous convergence analysis;
- Easier tuning of the control gains;
- Cooperative and competitive approaches as particular cases of the NSB.

The discussion of the properties above can be found in [2], [3]. Here it is of interest to consider new behaviors aimed at improve the observability in the sense described above.

A. The observable cooperative dive behavior

The key idea of the observable cooperative dive behavior is given in figure 5, at the beginning, both the vehicles are at the surface and both are GPS equipped.

Their absolute position is thus known and the initial error of the estimate of $\boldsymbol{p}$ can be considered as a Gaussian variable
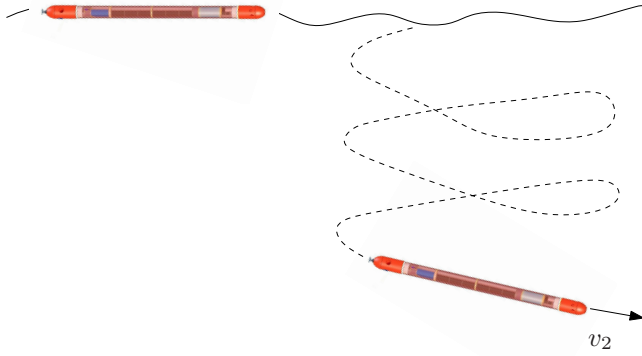
Fig. 5. The observable cooperative dive key idea. This movement guarantees full rank of the observability matrix and avoid the problems raised with the dive shown in Figure 3.

Fig. 6. A simple coordinated `move-to-goal` may be designed in order avoid lost of the observability properties, top view.

with null mean and variance related to the GPS sensor. The second vehicle can thus start its descend using an helix path in order to maintain a full rank observability matrix for the linearized system, this should guarantee that, once the desired depth is reached, the relative position error still is bounded. In addition, the helix path, or trajectory with an associated time law, is a trimming trajectory [17] and can be represented by the following equations:

$$\boldsymbol{p}_d(t) = \begin{bmatrix} \frac{v}{\dot\psi}\cos(\gamma)\sin(\dot\psi t) \\ -\frac{v}{\dot\psi}\cos(\gamma)\cos(\dot\psi t) \\ -vt\sin(\gamma) \end{bmatrix} \quad (8)$$

where $\dot\psi$ represents the yaw rate, γ the flight path angle and v the speed, supposed to be constant.

It is interesting to notice that an alternative cooperative dive can be achieved if the surface vehicle simply rotates on a circular path and the other vehicle dive vertically, i.e., with null pitch and roll angles.

B. The observable cooperative translation behavior

Figure 6 reports the key idea of the cooperative transaltion behavior. To avoid the singular configuration discussed above, the first vehicle is asked to advance with a *zig-zag* shape by following, e.g., a sinusoidal projection of a constant surge velocity on the inertial frame. The exact time law is not reported to preserve space, it is worth noticing that any movement *reach enough* with respect to the vehicles relative velocity can be defined as a proper cooperative translation behavior.

C. Merging different behaviors

All the behavioral approaches handle the concurrent action of different behaviors. The analytical study of this topic is out of the scope of the present paper, concerning the NSB, the reader may refer to [3] to deepen the approach. It is worth noticing that both the behaviors defined above need to be eventually considered together with an higher-level obstacle avoi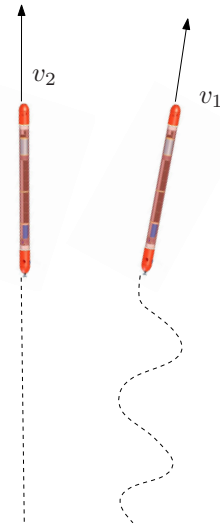dance behavior; from the observability perspective, however, the additional movement given by the avoidance of an obstacle can not decrease the full rank property imposed with the behavior above.

Focusing our attention on the movement on the horizontal plane, one possible hierarchy of concurrent behaviors might be:

1) Obstacle avoidance;
2) Observable cooperative translation;
3) Depth.

IV. NUMERICAL SIMULATIONS

Numerical simulations have been run to validate the proposed behavioral strategies. The vehicles tested is the Fòlaga [1] whose model can be described by:

$$\boldsymbol{M}(\varepsilon)\dot{\boldsymbol{\nu}} + \boldsymbol{C}(\boldsymbol{\nu},\varepsilon)\boldsymbol{\nu} + \boldsymbol{D}(\boldsymbol{\nu})\boldsymbol{\nu} + \boldsymbol{g}(\eta,\varepsilon) +$$
$$\boldsymbol{t}(\boldsymbol{\nu},\varepsilon)\dot{\boldsymbol{\varepsilon}} + \boldsymbol{f}(\boldsymbol{\nu},\boldsymbol{\eta},\dot{\boldsymbol{\varepsilon}}) + \boldsymbol{d} = \boldsymbol{\tau} \quad (9)$$

where, in addition to the common terms characterizing a rigid body submerged by a fluid [10], specific dynamic effects due to the water tank effect and battery desplacement can be recognized [1].

The vehicle's control take advantage from the possibility to move the battery pack and handle the ballast tank; those are independently and connected to the depth and pitch error via an external PID-control. Fòlaga is equipped with a main propeller and different water jet pumps. These pumps play the role of the common tunnel/transverse thrusters.

The unconstrained control allocation problem (see [10]) becomes:

$$\min_{u}\left(\boldsymbol{u}^{\mathrm{T}}\boldsymbol{W}\boldsymbol{u}\right), \quad \boldsymbol{W} > 0 \quad \text{subject to:} \quad \boldsymbol{\tau} = \boldsymbol{K}\boldsymbol{u} \quad (10)$$

where $\boldsymbol{u}$ is the actuator input and $\boldsymbol{K}$ is a map between

actuators and generalized forces $\boldsymbol{\tau}$:

$$\boldsymbol{K} = \begin{bmatrix} * & 0 & 0 & 0 & 0 \\ 0 & * & * & 0 & 0 \\ 0 & 0 & 0 & * & * \\ 0 & 0 & 0 & 0 & 0 \\ 0 & 0 & 0 & * & -* \\ 0 & -* & * & 0 & 0 \end{bmatrix} \quad (11)$$

where the star symbol denotes a non-null, positive value. The solution can be found easily using the generalized inverse:

$$\boldsymbol{u} = \boldsymbol{W}^{-1} \boldsymbol{K}^{\mathrm{T}} \left(\boldsymbol{K} \boldsymbol{W}^{-1} \boldsymbol{K}^{\mathrm{T}} \right)^{-1} \boldsymbol{\tau}. \quad (12)$$

A. Dive case study

In a first simulation study, the first vehicle is asked to dive following a vertical path, as described in section II-A and shown in Figure 3, and to surface back following the same path. The same dive is then achieved implementing the two observable cooperative dive behaviors defined in Section III-A followed, in this case too, by a surface under the same behavioral control. Figures 7 and 8 report the path for the sole descend; a similar path is achieved for the surfacing manoeuvre.

Fig. 8. Path of the vehicles during the second observable cooperative dive for the sole descend phase.

Figure 9 reports the measurements for the first cooperative dive and Figure 10 the estimation errors in terms of the norm of $\boldsymbol{p} - \hat{\boldsymbol{p}}$ during the three dives. As expected, the filter allows a correct estimation of the relative position between the vehicles only if unobservable configurations are avoided. Notice that, during the unobservable dive, the rank of the oservability matrix has been monitored and its 2-rank verified.
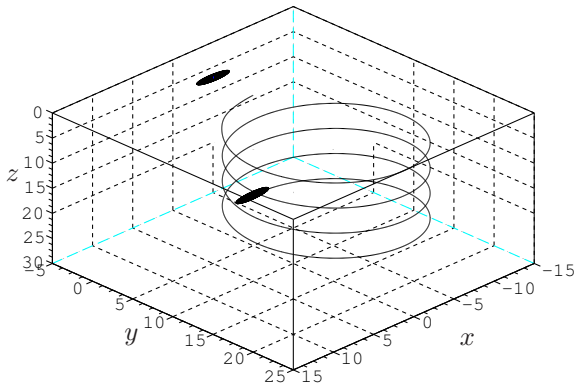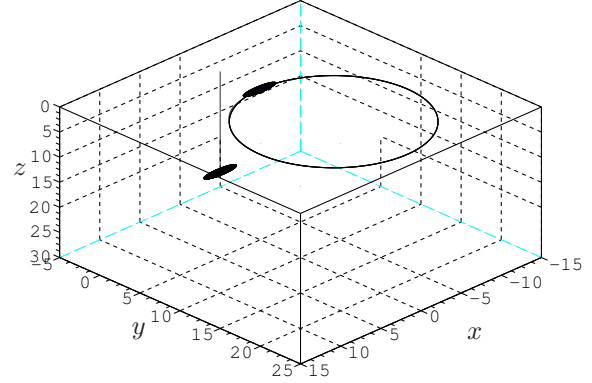
Fig. 7. Path of the vehicles during the first observable cooperative dive for the sole descend phase. Notice that one of the vehicles stays intentionally still.

An EKF is designed to estimate the relative position $\boldsymbol{p} \in \mathbb{R}^3$ with gains:

$$\begin{aligned} \boldsymbol{P} &= 0.2\boldsymbol{I}_3 \\ \boldsymbol{R}_w &= \mathrm{diag}\begin{bmatrix} 10 & 1 \end{bmatrix} \\ \boldsymbol{R}_v &= 0.1\boldsymbol{I}_3 \end{aligned} \quad (13)$$

where the matrix $\boldsymbol{P}$ is the covariance matrix of the estimation error, the matrix $\boldsymbol{R}_w$ is the covariance matrix of the measurement noise, the matrix $\boldsymbol{R}_v$ is the covariance matrix of the process noise and $\boldsymbol{I}_n$ is the $n \times n$ Identity matrix. The sensors are modeled as corrupted by Gaussian noise with zero mean and deviation standard of $1\,\mathrm{m}$ and $0.2\,\mathrm{m}$ for the distance and depth, respectively thus emulating the different performance of the sensors.
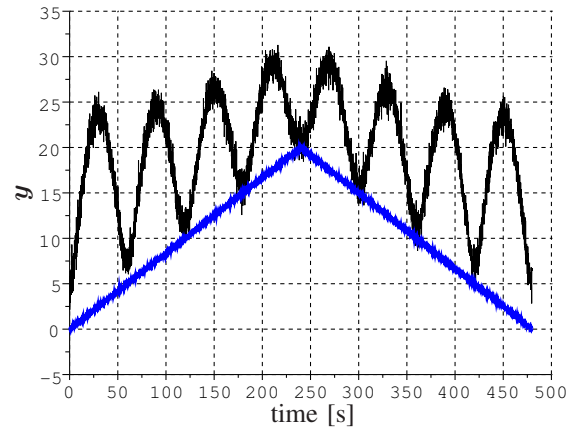
Fig. 9. Time history of the measurements during the first observable cooperative dive: distance (black) and depth (blue/gray).

Due to the similar performances of the two cordinated dives in terms of filter tracking error it is worht noticing that, in the first case, the surface vehicle stays still while the other is performing an helice path while, in the second case, the surface is following a circular path while the other is diving *simply*. It is of interest to include additional considerations such as, e.g., the controller performance, the energy consumption or the specific mission requirements, in order to finally select the appropriate dive behavior.
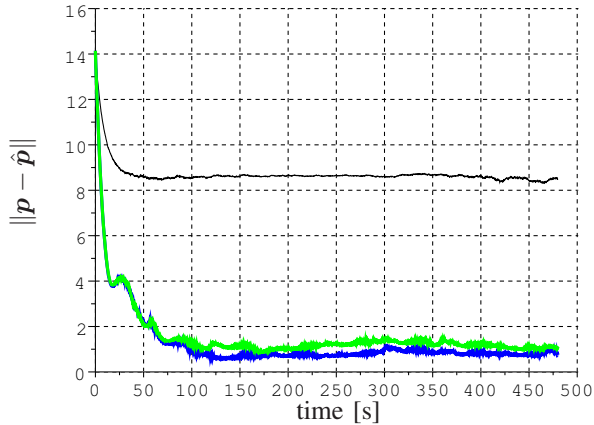
Fig. 10. Time history of the error norm during an not observable dive movement (black) and during the two observable cooperative dives (blue/light and green/lighter).

B. Translation case study

In a second simulation study, a cooperative translation is asked to the vehicles. Figure 11 reports time history of the error norm during an not observable translation movement (black) and during the observable cooperative translation (blue/gray). As expected, the not observable movement, in addition to the rank deficieny of the observability matrix, is not able to recover the initial error.
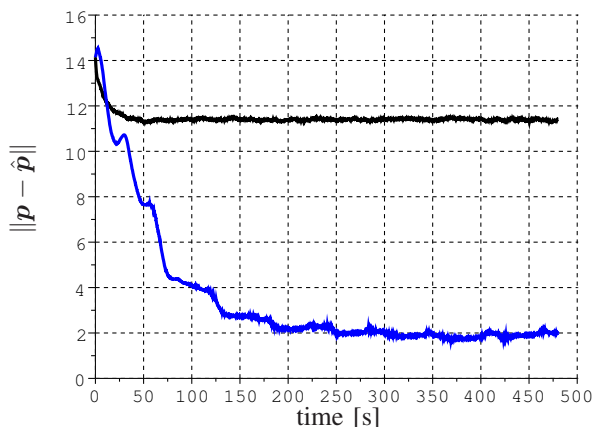

Fig. 11. Time history of the error norm during an not observable translation movement (black) and during the observable cooperative translation (blue/gray).

V. CONCLUSIONS

In this paper the effect of coordinated AUVs movements with respect to the problem of relative localization has been investigated. Proper definition of vehicle's behaviors allows to safely achieve movements such as, e.g., dive and cooperatively navigate in one direction. Numerical simulations on the mathematical model of the Fòlaga vehicle confirm the effectiveness of the proposed behaviors. Future developments include the experimental validation in open sea.

REFERENCES

[1] A. Alvarez, A. Caffaz, A. Caiti, G. Casalino, L. Gualdesi, A. Turetta, and R. Viviani. Fòlaga: A low-cost autonomous underwater vehicle combining glider and AUV capabilities. *Ocean Engineering*, 36(1):24–38, 2009.

[2] G. Antonelli. Stability analysis for prioritized closed-loop inverse kinematic algorithms for redundant robotic systems. *IEEE Transactions on Robotics*, 25(5):985–994, October 2009.

[3] G. Antonelli, F. Arrichiello, and S. Chiaverini. The Null-Space-based Behavioral control for autonomous robotic systems. *Journal of Intelligent Service Robotics*, 1(1):27–39, January 2008.

[4] G. Antonelli, F. Arrichiello, S. Chiaverini, and G. Sukhatme. Observability analysis of relative localization for auvs based on ranging and depth measurements. In *Proceedings 2010 IEEE International Conference on Robotics and Automation*, Anchorage, AK, May 2010.

[5] R.C. Arkin. Motor schema based mobile robot navigation. *The International Journal of Robotics Research*, 8(4):92–112, 1989.

[6] R.C. Arkin. *Behavior-Based Robotics*. The MIT Press, Cambridge, MA, 1998.

[7] A. Bahr, J.J. Leonard, and M.F. Fallon. Cooperative localization for autonomous underwater vehicles. *The International Journal Robotics Research*, 28:714–728, June 2009.

[8] P. Batista, C. Silvestre, and P. Oliveira. Necessary and sufficient conditions for the observability of linear motion quantities in strapdown navigation systems. In *Proceedings 2008 American Control Conference*, pages 1177–1182, St. Louis, MO, June 2009.

[9] R.A. Brooks. A robust layered control system for a mobile robot. *IEEE Journal of Robotics and Automation*, 2(1):14–23, 1986.

[10] T.I. Fossen. *Marine Control Systems: Guidance, Navigation and Control of Ships, Rigs and Underwater Vehicles*. Marine Cybernetics, Trondheim, Norway, 2002.

[11] R. Hermann and A. Krener. Nonlinear controllability and observability. *IEEE Transactions on Automatic Control*, 22(5):728–740, 1977.

[12] N. Kottege and U.R. Zimmer. Relative localisation for AUV swarms, in proceedings of the IEEE International Symposium on Underwater Technology 2007 (SUT'07). *Tokyo, Japan, April*, 2007.

[13] A.J. Krener. The convergence of the extended Kalman filter. *Lecture Notes in Control and Information Sciences*, pages 173–182, 2003.

[14] M.B. Larsen. Synthetic long baseline navigation of underwater vehicles. In *Proceedings MTS/IEEE Conference Oceans 2000*, pages 2043–2050, 2000.

[15] D.K. Maczka, A.S. Gadre, and D.J. Stilwell. Implementation of a cooperative navigation algorithm on a platoon of autonomous underwater vehicles. In *Proceedings MTS/IEEE Conference Oceans 2000*, pages 1–6, 2007.

[16] K. Reif, S. Gunther, E. Yaz, and R. Unbehauen. Stochastic stability of the discrete-time extended Kalman filter. *Automatic Control, IEEE Transactions on*, 44(4):714–728, Apr 1999.

[17] C. Silvestre. *Multi-Objective Optimization Theory with Applications to the Integrated Design of Controllers / Plants for Autonomous Vehicles*. PhD thesis, Instituto Superior Técnico, Lisboa, Portugal, 2000.

[18] S. Singh, M. Grund, B. Bingham, R. Eustice, H. Singh, and L. Freitag. Underwater acoustic navigation with the WHOI micro-modem. In *Proceedings MTS/IEEE Conference and Exhibition OCEANS 2000*, 2000.

[19] X.S. Zhou and S.I. Roumeliotis. Robot-to-robot relative pose estimation from range measurements. *IEEE Transactions on Robotics*, 24(6):1379–1393, Dec. 2008.